Journal of Radioanalytical and Nuclear Chemistry (2018) 317:315–323
https://doi.org/10.1007/s10967-018-5900-7

Synthesis and preliminary evaluation of ^{131}I-9-iodovinyl-tetrabenazine targeting vesicular monoamine transporter 2

Lihua Cao[1,2] · Minhao Xie[2] · Chao Zhao[1,2] · Jie Tang[2] · Chunyi Liu[2] · Yingjiao Xu[2] · Xiaomin Li[2] · Yi Liu[1] · Zhengping Chen[2]

Received: 26 January 2018 / Published online: 2 June 2018

Abstract

A new radioiodinated tetrabenazine (TBZ) derivative containing an iodovinyl group at 9-position of TBZ (^{131}I-IV-TBZ, **11a**) and the corresponding cold compound IV-TBZ (**11b**) were synthesized and characterized. Analysis of in vitro autoradiography with rat brain slices showed **11a** has a high uptake in the striatum and the uptake could be blocked by known vesicular monoamine transporter 2 (VMAT2) inhibitor. Furthermore, **11b** has a competitive binding to VMAT2. These results suggest that **11a** has ability to bind to VMAT2 and the binding is specific. Further studies are warranted to assess this radioiodinated TBZ derivative for VMAT2 imaging in vivo.

Keywords Tetrabenazine analogs · Synthesis · Vesicular monoamine transporter type 2 · Radioiodination · Autoradiography

Introduction

Vesicular monoamine transporter 2 (VMAT2), a member of the vesicular neurotransmitter transporter family, is responsible for transporting monoamine neurotransmitters (dopamine, norepinephrine and serotonin) into synaptic vesicles for subsequent storage and release [1, 2]. VMAT2 is found to be highly expressed in the central nervous system and pancreas beta cells [3–5]. Considerable evidences convincingly implicate that its alternation is associated with several neurological and psychiatric disorders such as Parkinson's disease (PD) [6–9]. These findings demonstrate that decrease of VMAT2 results in monoamine depletion and negative behavioral consequences, including bradykinesia, rigidity, postural instability and neurocognitive dysfunction, which are the characteristics of the PD patients. Moreover, reduction of VMAT2 in rat also causes the decrease of neurotransmitter and progressive neurodegeneration in multiple monoaminergic regions [10]. Thus, imaging VMAT2 in vivo or in vitro has provided a valuable measurement for tracing the function of monoaminergic neurons [11–13].

In recent decades, numerous efforts have been made to develop VMAT2 ligands for positron emission tomography (PET) in living body [14, 15], and some PET imaging agents targeting VMAT2 have been reported [16]. These VMAT2 imaging radiotracers are derived from tetrabenazine (TBZ) or its hydrogenated form dihydrotetrabenazine (DTBZ) (Fig. 1). For example, one useful TBZ derivative for imaging VMAT2 was ^{11}C-(+)-dihydrotetrabenazine (^{11}C-(+)-DTBZ, Fig. 1), which showed high affinity and selectivity to VMAT2 (Ki = 0.97 nM) [17]. However, the short half-life (20 min) of ^{11}C has precluded its widespread use. Then, fluoride[^{18}F], which has a relatively longer half-life (110 min) was used to label TBZ derivative, and ^{18}F-9-fluoropropyl-(+)-dihydrotetrabenazine (^{18}F-FP-(+)-DTBZ), with higher selectivity and affinity (Ki = 0.10 nM) to VMAT2 was developed [18]. Subsequent studies in rhesus monkeys demonstrated that

✉ Yi Liu
83775694@qq.com

✉ Zhengping Chen
chenzhengping@jsinm.org

[1] Jiangsu Key Laboratory of New Drug Research and Clinical Pharmacy, Xuzhou Medical University, Xuzhou 221004, China

[2] Key Laboratory of Nuclear Medicine, Ministry of Health, Jiangsu Key Laboratory of Molecular Nuclear Medicine, Jiangsu Institute of Nuclear Medicine, Wuxi 214063, China

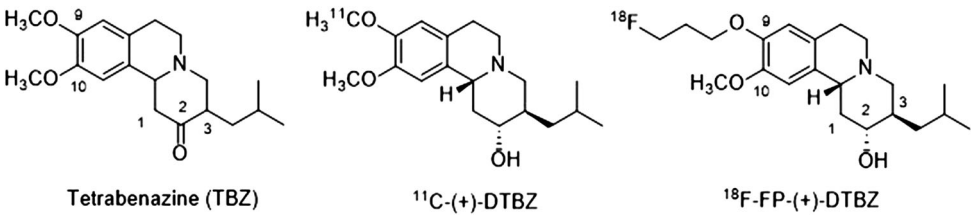

Fig. 1 Chemical structures of TBZ, ^{11}C-(+)-DTBZ and ^{18}F-FP-(+)-DTBZ

VMAT2 enriched brain region has a rapid and high brain uptake and retention of ^{18}F-FP-(+)-DTBZ. Human studies further indicates that ^{18}F-FP-(+)-DTBZ is a safe and effective VMAT2 imaging agent for clinical use [5, 19, 20].

Although PET is a useful method for noninvasive quantification of density and distribution of VMAT2, single photon emission computed tomography (SPECT) has some own advantages: First of all, it does not need an on-site cyclotron for synthesizing the imaging agent. Secondly, it is much cheaper and more widespread in clinic. Finally, radiopharmaceuticals for SPECT can be prepared conveniently from an optimized kit. Some ^{123}I or ^{99m}Tc labelled compounds for SPECT have been developed for brain imaging, providing good alternatives for PET brain imaging. For example, ^{123}I-N-(3-fluoropropyl)-2β-carbomethoxy-3β-(4-iodophenyl)nortropane (^{123}I-FP-β-CIT), a selective radiotracer binding to dopamine transporter, was developed for SPECT imaging, becoming a good substitute of ^{18}F-FP-CIT with PET [21].

With the development of VMAT2 radioligands for SPECT, an ^{123}I-labelling TBZ derivative with an iodovinyl at 2-position of the parent ring, 2-iodovinyl-TBZ, has been synthesized and evaluated for VMAT2 in early 1990s [22]. However, this radiotracer was not applied to SPECT imaging possibly due to that the 2-position of TBZ analog is a sensitive region for VMAT2 binding. It is noticed that the successful ^{18}F-FP-(+)-DTBZ has a fluoropropyl in the 9-position of DTBZ (Fig. 1) [23], suggesting good tolerance of the 9-position of TBZ analogs for VMAT2 binding. In the present study, we designed a new TBZ derivative with a 9-iodovinyl in TBZ ring, namely 9-iodovinyl-TBZ (IV-TBZ, **11b**), and completed its radioiodination for VMAT2 tracing. Due to non-availability of ^{123}I in our country, we substitute available ^{131}I for ^{123}I to perform an alternative initiatory investigation of ^{123}I-IV-TBZ. Herein, we report the synthesis, radiolabelling and preliminary evaluation of ^{131}I-IV-TBZ (**11a**) for VMAT2 measurement.

Experimental

Materials and methods

Compound 9-benzyloxy-TBZ (**5**) and TBZ was prepared in our lab according to the published methods [24]. ^{18}F-FP-(+)-DTBZ used in in vitro autoradiography, which was known as VMAT2 radioligand, was synthesized from tosylate precursor [25]. All other reagents and solvents were commercial products and used without further purification. MS spectra were acquired on a Waters SQ Detector 2 mass spectrometer. ^{1}H NMR and ^{13}C NMR spectra data were obtained from a Bruker Avance III Digital NMR Spectrometer (400 MHz for ^{1}H and 100 MHz for ^{13}C) with $CDCl_3$ as solvent. Chemical shifts were reported as δ values (parts per million) from an internal tetramethylsilane (TMS) resonance and coupling constants (*J*) were reported in hertz. Multiplicity is defined as s (singlet), d (doublet), t (triplet), m (multiplet), or dd (doublet of doublets). Analytical HPLC system was composed of a binary HPLC pump (Waters 1525, USA), a UV/visible detector (Waters 2487, USA) set at 280 nm and a flow scintillation analyzer (Radiomatic 610TR, Perkin-Elmer, USA). HPLC analysis was carried out on a C_{18} column (5 μm, 4.6 × 150 mm, Phenomenex) using acetonitrile/50 mmol (pH = 4.5) ammonium acetate aqueous solution (60:40, v/v) at a flow rate of 0.8 mL/min.

Male Sprague–Dawley rats weighing 180–200 g were used for the in vitro studies. The animal experiments were approved by the Animal Care and Ethics Committee of Jiangsu Institute of Nuclear Medicine.

Chemistry

3-Tri-n-butylstannyl-2-propen-1-ol (3) Tri-n-butyltin hydride (7 ml, 26 mmol **2**) was added dropwise to a mixture of propargyl alcohol (1 ml, 18.8 mmol **1**) and azobis (isobutyronitrile) (AIBN) (0.32 g, 1.94 mmol) at room temperature. After heating at 80 °C for 2 h, the reaction mixture was stirred for 1 h at room temperature. The crude product was purified by column chromatography on silica gel (ethyl acetate/hexane, 100/3, v/v) to yield as clear E-isomer oils of compound **3** (2.2 g, 38%). ^{1}H NMR (400 MHz, $CDCl_3$) *δ*: 6.08–6.33 (m, 2H), 4.16 (s, 2H), 1.75 (d, 1H), 1.54–1.46

(m, 6H), 1.35–1.26 (dq, J = 14.4, 7.3 Hz, 6H), 0.92–0.83 (m, 15H), ^{13}C NMR (100 MHz, $CDCl_3$), δ 7.71, 7.78, 9.42, 11.06, 11.13, 13.69, 27.01, 27.19, 27.56, 28.97, 29.07, 29.17, 66.34, 128.28, 147.08. MS (ESI) m/z: 291.20 $[M-CH_3(CH2)_3]^+$.

(E)-3-(tributylstannyl)allyl 4-methylbenzenesulfonate (4) Under N_2, to **3** (0.14 g, 0.41 mmol) in the dry ether (30 ml), at − 25 °C, potassium trimethylsilanolate (0.08 g, 0.64 mmol) was added. After stirring for 30 min, the p-toluenesulfonyl chloride was dissolved in dry ether and was added to the solution dropwisely. The resulting mixture was stirred at − 25 °C for 2 h. After the reaction mixture restore to the room temperature, the water layer was extracted with ethyl acetate. The combined organic layers was dried over anhydrous sodium sulfate, filtered, and concentrated to give the crude product, which was purified by hexane/ethyl acetate/trimethylamine (10/0.02/0.05, v/v) to yield product **4** as a colorless oil (60 mg, 30%). ^{1}H NMR (400 MHz, $CDCl_3$) δ: 7.80–7.76 (d, J = 8 Hz, 2H), 7.52–7.07 (d, J = 8 Hz, 2H), 6.25–6.35 (d, J = 20 Hz, 1H), 5.85–5.95 (dt, J = 4, 15 Hz, 1H), 4.81–4.35 (m, 2H), 2.45 (s, 3H), 1.52–1.36 (m, 6H), 1.37–1.17 (m, 6H), 0.96–0.76 (m, 15H). ^{13}C NMR (100 MHz, $CDCl_3$), δ 7.73, 7.87, 9.50, 11.11, 11,19, 13.66, 21.64, 26.95, 27.23, 27.51, 28.87, 28.98, 29.08, 73.33,127.96, 129.78, 133.61, 136.54, 139.01, 144.52. MS (ESI) m/z: 525.31 $[M + Na]^+$.

9-hydroxy-3-isobutyl-10-methoxy-1,3,4,6,7,11b-hexahydro-2H-pyrido[2,1-a]isoquinolin-2-one (6) A solution of compound **5** (0.43 g, 1.10 mmol) in ethanol (60 ml) was stirred at 30 min under N_2. Then 10 wt% palladium on carbon (0.15 g) was added and the mixture was hydrogenated with H_2 from hydrogen gas generator for 20 h at room temperature. The reaction mixture was heated at 50 °C to dissolve some of the product which had precipitated from the mixture and filtered to remove the catalyst. The filtrates was dried over anhydrous sodium sulfate and evaporated in vacuum to give a yellow orange solid. The crude product was purified ($CHCl_2$/MeOH, 10/0.05, v/v) by column chromatograph as afford **6** as a white solid product (0.10 g, 32.4%). ^{1}H NMR (400 MHz, $CDCl_3$) δ: 6.69 (s, 1H), 6.53 (s, 1H), 5.52 (s, 1H), 3.84 (s, 3H), 3.53–3.47 (m, 1H), 3.31–3.26 (dd, J = 8, 12 Hz, 1H), 3.15–3.03 (m, 2H), 2.90–2.86 (dd, J = 4, 8 Hz, 1H), 2.78–2.68 (m, 2H), 2.61–2.50 (m, 2H), 2.37–2.31 (t, J = 12 Hz, 1H), 1.85–1.75 (m, 1H), 1.70–1.62 (m, 1H), 1.09–0.99 (m, 1H), 0.92–0.90 (m, 6H); ^{13}C NMR (100 MHz, $CDCl_3$), δ: 22.08, 23.20, 25.40, 29.14, 35.06, 47.53, 47.72, 50.54, 56.01, 61.52, 62.56, 107.14, 114.37, 126.84, 128.06, 144.34. MS (ESI) m/z: 304.36 $[M + H]^+$.

(E)-3-isobutyl-10-methoxy-9-((3-(tributylstannyl)allyl)oxy)-1,3,4,6,7,11b-hexahydro-2H-pyrido[2,1-a]isoquinolin-2-one (10) To a mixture of compound **6** (0.20 g, 0.66 mmol) and **4** (0.50 g, 0.99 mmol) in dry acetone was added Cs_2CO_3 (1.61 g, 4.95 mmol). The resulting mixture was stirred at 60 °C for 4 h. After the reaction mixture was cooled down, the mixture was then quenched with H_2O (10 ml). The aqueous phase was extracted with ethyl acetate (3 × 10 ml). The combined organic extracted were dried over dry anhydrous sodium sulfate, evaporated and purified by flash column chromatography (hexane/ethyl acetate, 10/0.5, v/v) to afford 0.15 g as slight yellow powder of 35% yield. ^{1}H NMR (400 MHz, $CDCl_3$) δ: 6.62 (s, 1H), 6.55 (s, 1H), 6.36–6.30 (d, J = 20 Hz, 1H), 6.25–6.12 (dt, J = 4, 20 Hz, 1H), 4.63–4.60 (d, J = 4.0 Hz, 2H), 3.83 (s, 3H), 3.53–3.41 (m, 1H), 3.31–3.25 (dd, J = 4.0, 8.0 Hz, 1H), 3.16–3.0 (m, 2H), 2.96–2.86 (dd, J = 4, 12 Hz, 1H), 2.8–2.66 (m, 1H), 2.6–2.5 (m, 2H), 2.40–2.30 (m, 1H), 1.85–1.75 (m, 1H), 1.72–1,62 (m, 1H), 1.55–1.45 (m, 6H), 1.36–1,23 (m, 7H), 1.10–0.95 (m, 1H), 0.94–0.81 (m, 21H). ^{13}C NMR (100 MHz, $CDCl_3$), δ: 13.70, 22.08, 22.29, 22.72, 23.22, 25.39, 25.77, 27.27, 29.07, 29.71, 35.06, 40.59, 45.23, 47.56, 49.12, 50.61, 51.67, 56.03,59.73, 61.49, 62.08, 62.49, 72.50, 108.07, 113.70, 125.91, 128.07, 128.88, 132.07, 146.80, 147.81, 210.15. MS (ESI) m/z: 634.49 $[M + H]^+$.

(E)-3-iodoprop-2-en-1-ol (8) Under N_2, to compound (E)-ethyl-3-iodoacrylate **7** (0.71 g, 3.13 mmol) was dissolved in 5 ml dry dichloromethane at − 70 °C. Diisobutylaluminium hydride (6 ml, 1 M in hexane) was added dropwise for 60 min. The solution was allowed to warm up to 0 °C and quenched with 5 ml methanol, 10 ml methanol/H_2O (3:1), 5 ml H_2O, 20 ml dichloromethane and 15 ml potassium sodium tartrate solution (10% aqueous solution). The aqueous phase was extracted with dichloromethane (3 × 10 ml). The combined organic layers were dried over dry anhydrous sodium sulfate and evaporated to give the light yellow oil (0.48 g, 83%). The crude product can be moved to the next step without further purification.

(E)-3-iodoallyl 4-methylbenzenesulfonate (9) Compound **8** (0.48 g, 1.09 mmol), 1,2,2,6,6-Pentamethylpiperidine (0.25 g, 1.63 mmol, 0.30 ml) and p-Toluenesulfonic anhydride (0.36 mg, 1.09 mmol) were dissolved in 5 ml dry 1,2-dichloroethane and was stirred overnight at 50 °C under N_2. The solvent was evaporated and the residue dissolved in dichloromethane followed by addition of heptane. The resulting solution was filtered off and the filtrate was concentrated. The crude product was purified by flash column chromatography (hexane/ethyl acetate, 10/0.3, v/v) to afford compound **9** as a yellow oil (0.40 g, 45.0%). ^{1}H NMR (400 MHz, $CDCl_3$) δ: 2.46 (s, 3H), 4.44 (d, J = 4.0 Hz, 2H), 6.49 (d, J = 20 Hz, 1H), 6.65 (d, J = 8.0 Hz, 1H), 7.36 (d,

J = 4.0 Hz, 2H), 7.80(d, J = 8.0 Hz, 2H). ^{13}C NMR (100 MHz,$CDCl_3$), δ: 21.68, 70.79, 72.12, 83.26, 127.96, 129.98, 133.06, 133.95, 137.49, 145.15, MS (ESI) m/z: 483.57$[M + H]^+$+I + H_2O.

(E)-9-((3-iodoallyl)oxy)-3-isobutyl-10-methoxy-1,3,4,6,7,11b-hexahydro-2H-pyrido[2,1-a]isoquinolin-2-one (11b) To a solution of compound **6** (0.10 mg, 0.33 mmol) and compound **9** (0.16 mg, 0.49 mmol) in 20 ml dry acetone, Cs_2CO_3 (0.81 mg, 2.48 mmol) was added; the mixture was stirred for 6 h at 60 °C. After the reaction mixture was cooled down, water was added and the mixture was extracted with ethyl acetate. The combined organic layers was dried over dry anhydrous sodium sulfate, concentrated to give the crude product, which was purified by flash column chromatography (hexane/ethyl acetate, 10/2, v/v) to afford the cold compound as a solid powder (60 mg, 38.76%). ^{1}H NMR (400 MHz, $CDCl_3$) δ: 6.80–6.74 (d, J = 12.0 Hz, 1H), 6.61 (s, 1H), 6,57 (s, 1H), 6.54–6.50 (d, J = 16 Hz, 1H), 4.50–4.48 (d, J = 8.0 Hz, 2H), 3.82 (s, 3H), 3.52–3,49 (d, J = 12 Hz, 1H), 3.32–3.26 (d, J = 8 Hz, 1H), 3.16–3.02 (m, 2H), 2.92–2.88 (d, J = 4 Hz, 1H), 2.78–2.69 (m, 2H), 2.62–2.50 (m, 2H), 2.38–2.32 (d, J = 8 Hz, 1H), 1.84–1.77 (m, 1H), 1.71–1.63 (m, 1H), 1.07–1.00 (m, 1H), 0.94–0.87 (m, 6H). ^{13}C NMR (100 MHz, CDCl3) δ: 22.10, 23.19, 25.45, 29.28, 35.07, 47.56, 47.59, 50.53, 56.09, 61.51, 62.47, 70.91, 79.90, 108.57, 114.16, 126.18, 129.81, 140.76, 146.30, 148.15, 209.92. MS (ESI) m/z: 470.25 $[M + H]^+$.

Radiochemistry

The ^{131}I-labelled iodovinyl-TBZ derivative at 9-position, namely iodine[^{131}I]-*(E)-9-((3-iodoallyl)oxy)-3-isobutyl-10-methoxy-1,3,4,6,7,11b-hexahydro-2H-pyrido[2,1-a]isoquinolin-2-one* (**11a**), was prepared by an iododestannylation reaction. Aqueous hydrogen peroxide (100 µl, 3% w/v) was added to a vial containing compound **10** (100 µg) in 50 µl of EtOH, 100 µl of 0.4 N HCl, and 2 mCi $Na^{131}I$. The reaction proceeded at ambient temperature for 10 min, after which it was terminated by addition of 0.1 ml (300 mg/ml) sodium bisulfite. Then the reaction mixture was extracted with ethyl acetate. The crude product was purified with a semi-preparative HPLC on a C_{18} reversed-phase column eluted with acetonitrile/50 mmol (pH = 4.5) ammonium acetate aqueous solution (50:50, v/v) and detected with a radioactive detector. The radiochemical purity (RCP) of the compound **11a** was determined by HPLC with an isocratic solvent of acetonitrile/50 mmol (pH = 4.5) ammonium acetate aqueous solution (60:40, v/v) and co-injection of authentic compound **11b** was used to prove the identity of the produced ^{131}I-IV-TBZ. The specific activity (SA) of ^{131}I-IV-TBZ (**11a**) was measured by comparing the area of the UV peak of ^{131}I-IV-TBZ (**11a**) with a standard calibration curve of cold IV-TBZ (**11b**). The purified ^{131}I-IV-TBZ was used for the following in vitro autoradiography experiment. Stability of ^{131}I-IV-TBZ was tested in pH = 7.4 PBS buffer in a 37 °C incubator.

In vitro autoradiography studies

For in vitro autoradiography studies, Sprague–Dawley rats (180–200 g) under ether anesthesia were sacrificed and the brain rapidly removed. Coronal sections of 20 µm thickness were cut on a cryostat microtome at − 20 °C, thaw-mounted onto poly-lysine treatment glass slides, and stored at − 80 °C until use. Before autoradiography experiment, the brain sections were washed with ice-cold Tris-HCl buffer (50 mM/120 mM NaCl, pH = 7.4) for 40 min. Then, the sections were incubated in Tris-HCl-NaCl buffer containing 0.8 µCi/ml ^{131}I-IV-TBZ and ^{18}F-FP-(+)-DTBZ for 60 min at room temperature respectively. To determine the binding specificity of ^{131}I-IV-TBZ to VMAT2, 0.04 mM TBZ and cold compound (**11b**) were added to block the binding of ^{131}I-IV-TBZ and ^{18}F-FP-(+)-DTBZ, respectively. The sections were washed three times with ice-cold Tris-HCl buffer. The dried tissue sections were then exposed to the imaging plate for 1 h and analyzed with the phosphor imager (OptiQuant, 5.0.0.2, Perkin Elmer).

Partition coefficients

Partition coefficients were measured by mixing minimal volume of pure ^{131}I-IV-TBZ with 3 ml n-octanol and 3 ml PBS buffer (pH 7.0, 0.01 M phosphate) in a test tube. The mixture was vortexed for 3 min at room temperature and then centrifuged at 6000 rpm for 10 min. Two samples (1 ml each) from the 1-octanol and the buffer layers were taken and counted in a Wizard2 2480 gamma counter (Perkin-Elmer, USA). The partition coefficient was calculated from the ratio of counts per minute (CPM) of the 1 ml n-octanol to that of buffer. Then, another 1 ml of 1-octanol layer were mixed with 2 ml n-octanol and 3 ml buffer and repartitioned until consistent partitions of coefficient values were obtained. The measurement was repeated for three times.

Results and discussion

Chemistry and radiochemistry

The syntheses of ^{131}I-IV-TBZ (**11a**) and its precursor 9-tributylstannylethenyl-TBZ (**10**) are shown in Scheme 1. Compound **3** with E-configuraton was prepared by

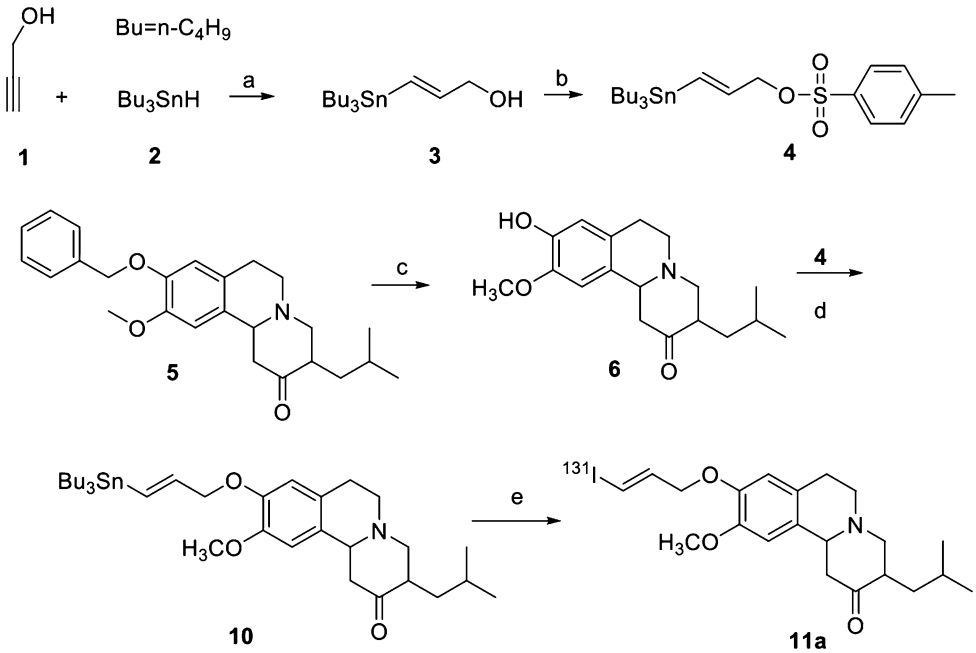

Scheme 1 Synthesis of the radiolabelled compound ^{131}I-IV-TBZ (**11a**) and its precursor compound **10**. (**a**) AIBN; (**b**) Tosyl chloride; (**c**) Pd-C/H_2; (**d**) Cs_2CO_3, acetone; (**e**) Na^{131}I, H_2O_2

treatment of propargyl alcohol (**1**) and tri-butyltin hydride (**2**) in a proper proportion (1:1.5) with a catalytic amount of azobis (isobutyronitrile) at a 30% yield as a colorless oil. Subsequently, treatment of an ether solution of the resulting hydroxyl of compound **3** intermediate with p-toluenesulfonyl chloride and potassium trimethylsilanolate afforded compound **4**. ^{1}HNMR for structure confirmation of compound **3** and **4** were consistent with the reported data [26]. Simultaneously, the racemic benzyl ether **5** was selectively hydrogenated with 10 wt% palladium/carbon to produce phenol **6** as described previously [27]. Finally, the tributyltin precursor **10** was prepared by reacting compound **6** and **4** with cesium carbonate at a yield of 35%. The coupling constants observed for the vinyl protons of compound **10** (J = 20 Hz) was comparable with the trans conformation [28].

To synthesis the cold compound IV-TBZ (**11b**), we had tried to utilize the precursor **10** to react with I_2 directly to obtain the product. Unfortunately, the reaction gave an unexpected product with a smaller molecular weight of MW_{11b}—2 (reducing two hydrogen of **11b**). We speculated that the reaction generated a double bond at the C11b position of tetrabenazine ring so that the nitrogen ring and the carbonyl group consist of conjugated π system. Our group has previously found the formation of the double bond on C11b in a similar reaction of synthesizing TBZ analogs [29]. Therefore, to obtain the cold compound **11b** as a reference of the radiolabelled ^{131}I-IV-TBZ, we designed a different synthetic route as illustrated in Scheme 2. Firstly, the ester **7** with E-configuration was reacted with a reducing agent diisobutylaluminium hydride to produce the propenol **8** [30]. Then, the hydroxyl of compound **8** was mesylated with 4-toluenesulphonic anhydride and 1,2,2,6,6-pentamethylpiperidine in 1,2-dichloroethane under reflux to generate the intermediate **9**. Finally, the cold compound (**11b**) was synthesized by reaction of compound **9** and phenol **6**, in which the p-toluene sulfonyl group of **9** was substituted with **6** through Cs_2CO_3 in acetone solvent. Compound **11b** was obtained in 38.7% yield with an E-configuration as the starting reactant ester **7**. As indicated by ^{1}HNMR spectral analysis, compound **11b** exhibited a doublet centered at δ 6.54 for the proton germinal to the iodine with a coupling constant J = 16 Hz and a doublet centered at δ 6.80 for the trans vinylic proton germinal to the methylene with the coupling constant J = 12 Hz, which are comparable to the E-configuration of a iodoethenyl compound reported by Mark et al. [31].

The final product ^{131}I-IV-TBZ was prepared by Na^{131}I treatment of the tributyltin precursor **10** under H_2O_2 and HCl. It is assumed that the compound **10** was reacted with I^+ generated in situ by H_2O_2 in acid condition. We found that pH value is a key factor of the radiolabelling reaction to get high yield of ^{131}I-IV-TBZ. A slight acidic environment (pH 2–3) gave ~ 80% radioiodinated product, whereas other pH range solution gave dramatically lower radiolabeling yield. That is, the radiochemical yield was about 80% under the optimized condition. The crude product of **11a** was purified by HPLC to give a radiochemical purity of 96%, with the same retention time of the cold compound **11b** (Fig. 2), validating the same structure to the cold compound IV-TBZ. SA of the purified **11a** was 850 ± 140 Ci/mmol as determined with analytical HPLC under the same condition of RCP. Stability test showed that

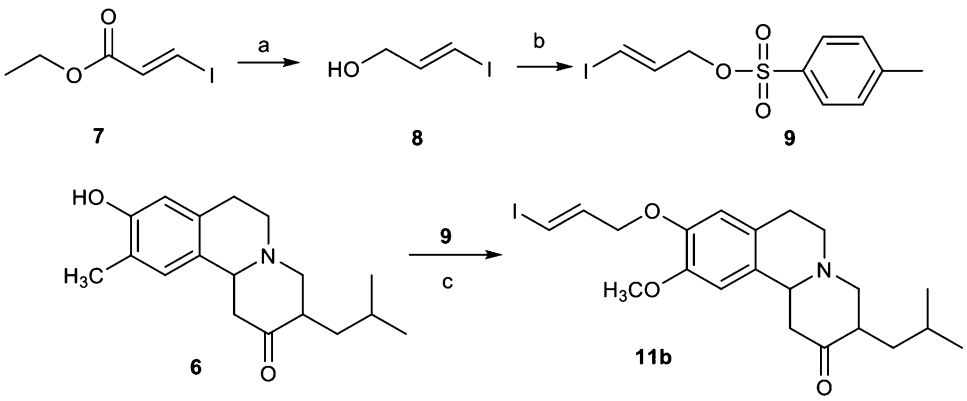

Scheme 2 Synthesis of the cold compound IV-TBZ (**11b**). (**a**) DIBAL; (**b**) 4-Toluenesulphonic anhydride; (**c**) Cs_2CO_3

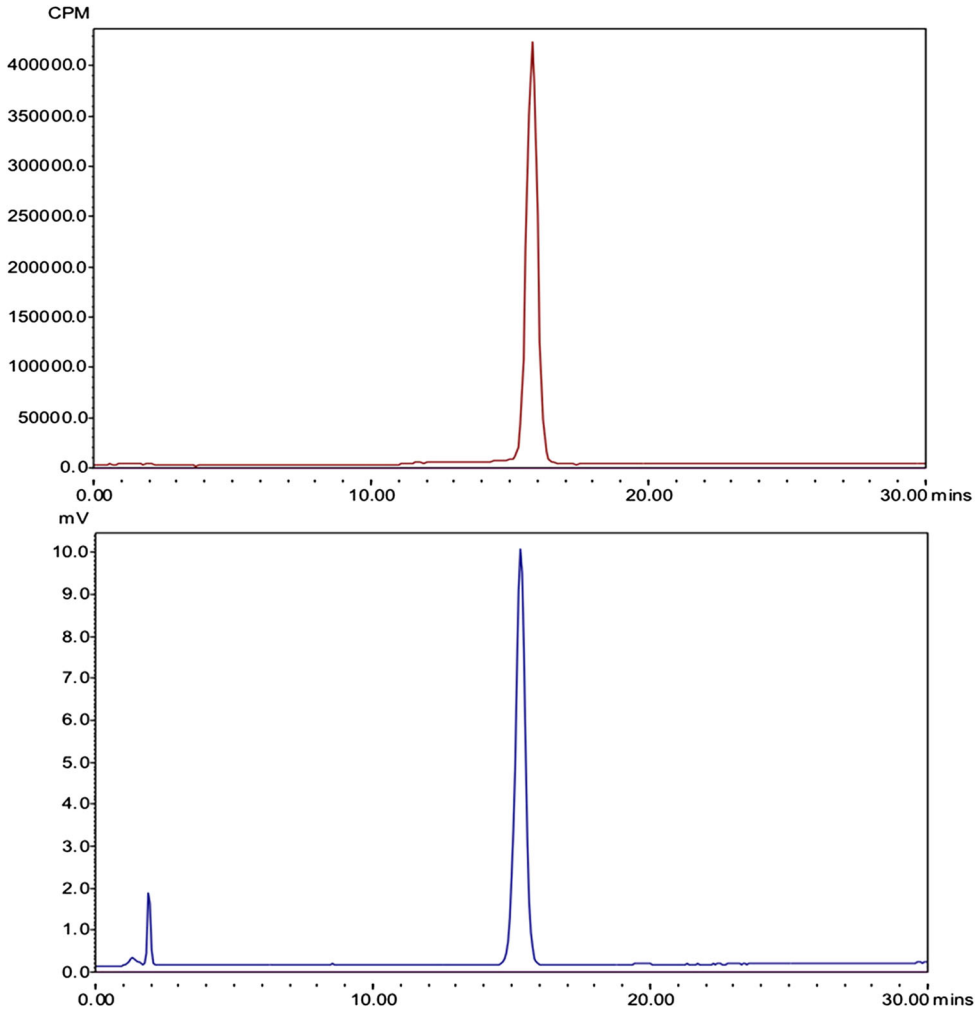

Fig. 2 HPLC analysis of compound ^{131}I-IV-TBZ (**11a**) with a radiation detector (upper) and coinjection of nonradioactive IV-TBZ (**11b**) with a UV detector (bottom)

the radioiodinated ligand **11a** retained a RCP of ~ 95% as long as 24 h at 37 °C in pH = 7.4 PBS buffer, assuring its application in further pharmacological studies.

In vitro autoradiography

The technology of in vitro autoradiography can detect the binding characteristic of radioactive ligand in organs and tissues sensitively. In this study, the localization of ^{131}I-IV-TBZ in brain slices was investigated via in vitro autoradiography to assess its binding ability and specificity to

VMAT2. The images gave a good degree of anatomical resolution of the striatum as shown in Fig. 3a–d.

To assess the ability of ^{131}I-IV-TBZ to bind to VMAT2, in vitro autoradiography was performed with rat brain slices. As shown in Fig. 3b, the striatum (ST), which is the VMAT2 most enriched region of the brain, was clearly delineated after incubated with ^{131}I-IV-TBZ while the cortex (CX), a nontarget region containing a minimal amount of VMAT2, was recognized as background at the same condition. Ratio of striatum to cortex (ST/CX) reached to 2.71 ± 0.55 (n = 3). This ratio is comparable with ^{18}F-FP-(+)-DTBZ, a known VMAT2 ligand with high affinity and specificity [25], which gave a similar image of autoradiography (Fig. 3a) and a ratio of ST/CX of 3.86 ± 0.21 (n = 3) under the same condition. These results suggested that ^{131}I-IV-TBZ may has a similar binding ability as ^{18}F-FP-(+)-DTBZ, that is, ^{131}I-IV-TBZ possibly binds to VMAT2 specifically. To confirm this, a VMAT2 inhibitor TBZ [32] was added to ^{131}I-IV-TBZ solution in in vitro autoradiography. Quantitative analysis showed a dramatic decrease of radioactivity level in the striatum as compared to ^{131}I-IV-TBZ alone (Fig. 3b, d). Ratio of ST/CX was decreased from 2.71 ± 0.55 to 1.18 ± 0.17 ($P < 0.05$, Fig. 3e), suggesting that uptake of ^{131}I-IV-TBZ in the striatum can be blocked by VMAT2 inhibitor. These results indicated that ^{131}I-IV-TBZ binds to VMAT2 specifically in rat brain.

To furtherly validate specificity of ^{131}I-IV-TBZ to VMAT2, blocking effect of the cold IV-TBZ (**11b**) to the known VMAT2 ligand ^{18}F-FP-(+)-DTBZ was also evaluated. As shown in Fig. 3a, c, a dramatic decrease of the specific uptake of ^{18}F-FP-(+)-DTBZ in the striatum was observed when combined with IV-TBZ. A significant decrease of ST/CX ratio of IV-TBZ blocking samples was demonstrated (ST/CX = 1.59 ± 0.23 for ^{18}F-FP-(+)-DTBZ combined with IV-TBZ and ST/CX = 3.86 ± 0.21 for ^{18}F-FP-(+)-DTBZ alone. $P < 0.01$ Fig. 3e), implying that compound IV-TBZ (***11b***) has competitive capability to the known VMAT2 ligand ^{18}F-FP-(+)-DTBZ [25]. Since ^{131}I-IV-TBZ has the same chemical structure of the cold IV-TBZ, we can infer that ^{131}I-IV-TBZ has a selective binding to VMAT2.

In summary, results of the above in vitro autoradiography analysis preliminarily suggested that ^{131}I-IV-TBZ has

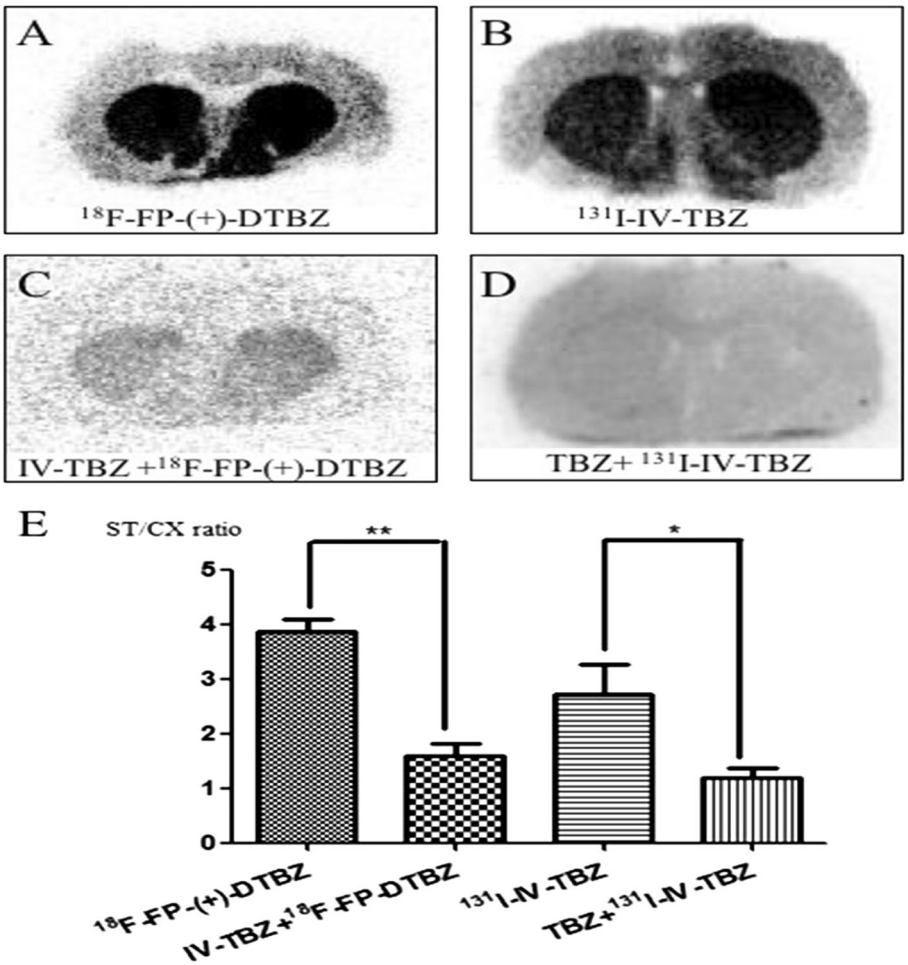

Fig. 3 In vitro autoradiographic images of representative rat brain striatum sections labelled with **a** ^{18}F-FP-(+)-DTBZ, **b** ^{131}I-IV-TBZ, **c** ^{18}F-FP-(+)-DTBZ combined with IV-TBZ, **d** ^{131}I-IV-TBZ combined with TBZ and **e** ratio of ST/CX of quantitative analysis from image a, b, c and d. Data are expressed as mean ± SD (n = 3). $^{**}P < 0.01$; $^{*}P < 0.05$

a binding specificity to VMAT2. One limitation of our research is the absence of in vivo experiments. A potential challenge is the ability of ^{131}I-IV-TBZ to cross the blood brain barrier (BBB) for in vivo assessment. However, the partition coefficient value of Log $P_{o/b}$ = 1.75 (pH = 7.0) suggests that ^{131}I-IV-TBZ can be delivered to the brain for tracing VMAT2. Biodistribution of ^{131}I-IV-TBZ and SPECT imaging with alive animals may further elucidate the in vivo characteristics of this radioiodinated ligand.

Conclusions

A new radioiodinated TBZ derivative ^{131}I-IV-TBZ (**11a**), its corresponding precursor (**10**) and cold compound (**11b**) were synthesized and characterized. In vitro autoradiography and blocking studies demonstrated specific binding of ^{131}I-IV-TBZ to VMAT2 in the striatum of rat brain slices. These preliminary results suggested that ^{131}I-IV-TBZ may be a potential radioiodinated candidate for VMAT2 measurement. Our studies with the isotope ^{131}I provide a reference to furtherly develop ^{123}I-labelled TBZ derivatives as a VMAT2 SPECT imaging agent.

Acknowledgements The present work was supported by the National Key R&D Program of China (2016YFC1306600), the National Natural Science Foundation of China (81671723), the Jiangsu Provincial Natural Science Foundation (BK20161138), the Wuxi Municipal Commission of Health and Family Planning (Q201631), the Open Program of Key Laboratory of Nuclear Medicine, Ministry of Health and Jiangsu Key Laboratory of Molecular Nuclear Medicine (KF201503) and the Program for Jiangsu Provincial High-Level Talents in Six Major Industries (2016-WSN-037).

References

1. Lohr KM, Bernstein AI, Stout KA, Dunn AR, Lazo CR, Alter SP, Wang M, Li Y, Fan X, Hess EJ (2014) Increased vesicular monoamine transporter enhances dopamine release and opposes Parkinson disease-related neurodegeneration in vivo. Proc Natl Acad Sci USA 111(27):9977–9982
2. Yang C-T, Ghosh KK, Padmanabhan P, Langer O, Liu J, Halldin C, Gulyás BZ (2017) PET probes for imaging pancreatic islet cells. Clin Transl Imaging 5(6):507–523
3. Cliburn RA, Dunn AR, Stout KA, Hoffman CA, Lohr KM, Bernstein AI, Winokur EJ, Burkett J, Schmitz Y, Caudle WM, Miller GW (2017) Immunochemical localization of vesicular monoamine transporter 2 (VMAT2) in mouse brain. J Chem Neuroanat 83–84:82–90
4. Lin SC, Lin KJ, Hsiao IT, Hsieh CJ, Lin WY, Lu CS, Wey SP, Yen TC, Kung MP, Weng YH (2014) In vivo detection of monoaminergic degeneration in early parkinson disease by ^{18}F-9-Fluoropropyl-(+)-Dihydrotetrabenzazine PET. J Nucl Med 55(1):73–79
5. Wood H (2014) Parkinson disease: ^{18}F-DTBZ PET tracks dopaminergic degeneration in patients with Parkinson disease. Nat Rev Neurol 10(6):305
6. Luk KC, Kehm V, Carroll J, Zhang B, O'Brien P, Trojanowski JQ, Lee VMY (2012) Pathological α-synuclein transmission initiates Parkinson-like neurodegeneration in non-transgenic mice. Science 338(6109):949–953
7. De LF-FR, Furtado S, Guttman M, Furukawa Y, Lee CS, Calne DB, Ruth TJ, Stoessl AJ (2003) VMAT2 binding is elevated in dopa-responsive dystonia: visualizing empty vesicles by PET. Synapse 49(1):20–28
8. Chen MK, Hiroto K, Yun Z, Adams RJ, Brašić JR, Mcglothan JL, Tatyana V, Burton NC, Mohab A, Anil K (2008) VMAT2 and dopamine neuron loss in a primate model of Parkinson's disease. J Neurochem 105(1):78–90
9. Zheng G, Dwoskin LP, Crooks PA (2006) Vesicular monoamine transporter 2: role as a novel target for drug development. AAPS J 8(4):E682–E692
10. Hall FS, Itokawa K, Schmitt A, Moessner R, Sora I, Lesch KP, Uhl GR (2014) Decreased vesicular monoamine transporter 2 (VMAT2) and dopamine transporter (DAT) function in knockout mice affects aging of dopaminergic systems. Neuropharmacology 76(2):146–155
11. Taylor TN, Caudle WM, Miller GW (2011) VMAT2-deficient mice display nigral and extranigral pathology and motor and nonmotor symptoms of Parkinson's disease. Parkinsons Dis 10(supplement 4):124–165
12. Weng CC, Huang SL, Chen ZA, Lin KJ, Hsiao IT, Yen TC, Kung MP, Wey SP, Hsu CH (2017) [^{18}F]FP-(+)-DTBZ PET study in a lactacystin-treated rat model of Parkinson disease. Ann Nucl Med 31(7):506–513
13. Chang CC, Hsiao IT, Huang SH, Lui CC, Yen TC, Chang WN, Huang CW, Hsieh CJ, Chang YY, Lin KJ (2015) ^{18}F-FP-(+)-DTBZ positron emission tomography detection of monoaminergic deficient network in patients with carbon monoxide related parkinsonism. Eur J Neurol Off J Eur Fed Neurol Soc 22(5):845–852
14. Kilbourn MR (2014) Radioligands for imaging vesicular monoamine transporters. PET and SPECT of neurobiological system. Springer, Berlin
15. Wu X, Cai H, Ran G, Lin L, Jia Z (2014) Recent progress of imaging agents for Parkinson's disease. Curr Neuropharmacol 12(6):551–563
16. Zhu L, Ploessl K, Kung HF (2014) PET/SPECT imaging agents for neurodegenerative diseases. Chem Soc Rev 43(19):6683–6691
17. Kilbourn M, Lee L, Borght TV, Jewett D, Frey K (1995) Binding of a-dihydrotetrabenazine to the vesicular monoamine transporter is stereospecific. Eur J Pharmacol 278(3):249–252
18. Goswami R, Ponde DE, Kung MP, Hou C, Kilbourn MR, Kung HF (2006) Fluoroalkyl derivatives of dihydrotetrabenazine as positron emission tomography imaging agents targeting vesicular monoamine transporters. Nucl Med Biol 33(6):685–694
19. Lin KJ, Weng YH, Wey SP, Hsiao IT, Lu CS, Skovronsky D, Chang HP, Kung MP, Yen TC (2010) Whole-body biodistribution and radiation dosimetry of ^{18}F-FP-(+)-DTBZ (^{18}F-AV-133): a novel vesicular monoamine transporter 2 imaging agent. J Nucl Med 51(9):1480–1485
20. Hsiao IT, Weng YH, Hsieh CJ, Lin WY, Wey SP, Kung MP, Yen TC, Lu CS, Lin KJ (2014) Correlation of Parkinson disease severity and ^{18}F-DTBZ positron emission tomography. JAMA Neurol 71(6):758–766
21. Sixeldöring F, Liepe K, Mollenhauer B, Trautmann E, Trenkwalder C (2011) Samenvatting the role of ^{123}I-FP-CIT-SPECT in the differential diagnosis of Parkinson and tremor syndromes: a critical assessment of 125 cases. J Neurol 258(12):2147–2154
22. Canney DJ, Guo YZ, Kung MP, Kung HF (1993) Synthesis and preliminary evaluation of an iodovinyl-tetrabenazine analog as a

marker for the vesicular monoamine transporter. J Label Compd Radiopharm 33(4):355–368
23. Zhu L, Liu Y, Plossl K, Lieberman B, Liu J, Kung HF (2010) An improved radiosynthesis of [^{18}F]AV-133: a PET imaging agent for vesicular monoamine transporter 2. Nucl Med Biol 37(2):133–141
24. Liu C, Chen Z, Li X, Tang J, Qin X (2013) (+)-9-Benzyloxy-α-dihydrotetrabenazine as an important intermediate for the VMAT2 imaging agents: absolute configuration and chiral recognition. Chirality 25(4):215–223
25. Tsao HH, Lin KJ, Juang JH, Skovronsky DM, Yen TC, Wey SP, Kung MP (2010) Binding characteristics of 9-fluoropropyl-(+)-dihydrotetrabenzazine (AV-133) to the vesicular monoamine transporter type 2 in rats. Nucl Med Biol 37(4):413–419
26. Tamagnan GD, Alagille D, Costa HD (2009) Compounds and amyloid probes thereof for therapeutic and imaging uses. U.S. Patent 20100150833, 17-2-2010
27. Boldt K, Brine G, Rehder K (2008) Synthesis of (+)-9-O-desmethyl-α-dihydrotetrabenazine, precursor for the high affinity VMAT2 imaging PET radioligand ^{11}C-(+)-α-dihydrotetrabenazine. Org Prep Proced 40(4):379–384
28. Musachio JL, Lever JR (1989) Radioiodination via vinylstannylated alkylating agents. Tetrahedron Lett 30(28):3613–3616
29. Xue D, Liu C, Li X, Tang J, Cao L, Liu Y, Chen Z (2017) Structural requirement of C11b chirality of tetrabenazine analogs as VMAT2 imaging ligands: synthesis and in vivo evaluation. J Radioanal Nucl Chem 313(2):419–428
30. Rami-Mark C, Bornatowicz B, Fink C, Otter P, Ungersboeck J, Vraka C, Haeusler D, Nics L, Spreitzer H, Hacker M (2013) Synthesis, radiosynthesis and first in vitro evaluation of novel PET-tracers for the dopamine transporter: ^{11}C-IPCIT and ^{18}F-FE@IPCIT. Bioorg Med Chem 21(24):7562–7569
31. Goodman MM, Chen P, Plisson C, Martarello L, Galt J, Votaw JR, Kilts CD, Malveaux G, Camp VM, Shi B (2003) Synthesis and characterization of iodine-123 labeled 2β-carbomethoxy-3β-(4'-((Z)-2-iodoethenyl)phenyl)nortropane. A ligand for in vivo imaging of serotonin transporters by single-photon-emission tomography. J Med Chem 46(6):925–935
32. Guay DR (2010) Tetrabenazine, a monoamine-depleting drug used in the treatment of hyperkinetic movement disorders. Am J Geriatr Pharm 8(4):331–373